Assiut University Journal of Multidisciplinary Scientific Research (AUNJMSR)
Faculty of Science, Assiut University, Assiut, Egypt.
Printed ISSN 2812-5029
Online ISSN 2812-5037
Vol. 54(2): 280-302 (2025)
https://aunj.journals.ekb.eg

Histopathological Study of Kidney and Lung induced by *Acanthamoeba polyphaga* Infection in Immunosuppressed Mice

Mona M. Khalaf[1], Sara S. Abdel-Hakeem[1], Mahmoud Abdel-Zaher Abdel-Samiee[2], Gamal Hassan Abed[1], Fatma A. S. Anwar[1]

[1]Parasitology Laboratory, Zoology and Entomology Department, Faculty of Science, Assiut University (71526), Assiut, Egypt.

[2]Department of Pathology and Clinical Pathology, Faculty of Veterinary Medicine, Assiut University (71526), Assiut, Egypt.

[*]Corresponding Author: mona_khalaf20@science.aun.edu.eg

ARTICLE INFO

Article History:
Received: 2024-12-08
Accepted: 2025-02-10
Online: 2025-04-27

Keywords:

Acanthamoeba polyphaga, Histopathology, Mice, Pathogenicity, Kidney, Lung

ABSTRACT

This study evaluated the pathogenicity of *Acanthamoeba polyphaga* in immunosuppressed mice, focusing on its histopathological effects on the kidneys and lungs. Fifty male Swiss albino mice were divided into three groups: immunosuppressed uninfected (CS), immunosuppressed *Acanthamoeba polyphaga* infected (AS), and negative control (C). The CS and AS groups were sacrificed at 2, 7, and 15 days post-infection (dpi). Histopathological analysis of infected kidneys revealed inflammatory cell infiltration in the renal cortex including periglomerular, perivascular, and interstitial tissues, which was evident at 2 and 7 dpi. Additionally, necrosis in the tubular epithelium nuclei was observed more evident at 15 dpi and distribution of parasite stages in the periglomerular and perivascular areas. The parasite was successfully re-isolated from freshly dissected infected kidney tissues at 2 dpi. Physiological assessment indicated a significant increase in renal biomarkers (urea and creatinine) at 7 and 15 dpi. In the lungs, histopathological findings included perivascular inflammatory cell

infiltration, thickening of alveolar septae (a pathognomonic lesion for pneumonia), and congestion in the blood vessels at 7 and 15 dpi. However, lung tissues showed negative results in the re-isolation test. These findings highlight the systemic pathogenic potential of *A. polyphaga* in immunosuppressed hosts, particularly its pronounced impact on histopathology and renal function and moreover, its presence and impact on lung tissues.

INTRODUCTION

Opportunistic infections caused by *Acanthamoeba* spp., pathogenic free-living amoebae, pose significant health risks, particularly to immunocompromised individuals [1]. *Acanthamoeba* spp. are widely distributed across various environments, including soil, water, and other environmental niches. In Egypt, *Acanthamoeba* spp. have been detected in multiple water sources such as the Nile River, tap water, and swimming pools [2-4]. Additionally, they have been isolated from cosmetic lenses and disinfectant solutions, as well as in hemodialysis and dental units, and several cases of *Acanthamoeba keratitis* (AK) have been reported, primarily associated with contact lens use [5-7]. Furthermore, in another country, *Acanthamoeba* spp. have been found in throat swabs of healthy individuals, indicating their potential presence in ordinary household environments [8].

These amoebae are primarily known to target the central nervous system (CNS), causing granulomatous amoebic encephalitis (GAE). Moreover, they can disseminate to various organs, including the kidneys, liver, and lungs, often leading to multi-organ failure and high mortality [9-11]. High-risk in these cases include patients undergoing intensive steroid therapy, organ transplant recipients, individuals infected with HIV, and children [12]. In addition, even in healthy individuals, these amoebae can cause extracerebral infections, such as *Acanthamoeba keratitis* (AK), which affects the cornea of the eye and may lead to vision loss [13]. Disseminated infections by *Acanthamoeba* may occur through intranasal penetration during the inhalation of contaminated air/ water, or via skin lesions containing invasive forms [14, 15]. *Acanthamoeba* spp.

demonstrate remarkable adaptability, targeting specific organs or causing widespread systemic infections depending on host factors and the amoebic strain [16]. Disseminated Acanthamoebiasis is often under-recognized in immunosuppressed patients which spreads hematogenous and proves fatal in transplant recipients [17, 18]. Patients with GAE may have pneumonia, this was reported in a child with congenital immunodeficiency and also in a lung transplant patient [19, 20, 21]. Furthermore, *Acanthamoeba* spp. have been recovered from the kidney of a Korean child diagnosed with meningoencephalitis [22].

One of the contributing factors to kidney diseases is the parasitic infection. Animal studies have shown that amoebae travel through the bloodstream and infiltrate the kidneys, leading to their dysfunction [1]. However, the precise mechanisms by which parasites cause kidney damage remain poorly understood, complicating the development of targeted treatments. This challenge is further exacerbated by the long-term and delayed impact of the infections on kidney tissue [23]. Additionally, repeated exposure to *Acanthamoeba* trophozoites through the nasal cavity can trigger allergic airway inflammation. These amoebas have the ability to penetrate mucosal membranes and break down natural barriers, such as the blood-brain barrier, making the nasal cavity particularly vulnerable to infection [24, 25]. Hence, this paper aims to highlight the potential of *A. polyphaga* to induce histopathological changes in the kidney and lungs of immunosuppressed mice, providing insights into the pathogenic mechanisms of *Acanthamoeba* infections.

MATERIALS AND METHODS

2.1. Isolation and cultivation of *Acanthamoeba polyphaga* strain

The *A. polyphaga* strain was previously isolated from contaminated cosmetic, new, and used contact lenses and identified both morphologically and molecularly as belonging to the T4 genotype (GenBank OL336326.1) at the Parasitology Laboratory, Zoology Department, Faculty of Science, Assiut University, Egypt [6].

2.2. Animals and Ethics

The experimental procedures were approved by the Ethical Committee of the Faculty of Science, Assiut University, Assiut, Egypt (FSREC) (Approval No. 01-2024-0001). The study adhered to Egyptian regulations and university guidelines concerning the ethical treatment of experimental animals and followed the ARRIVE (Animals in Research: Reporting In Vivo Experiments) guidelines [26]. A total of 50 male Swiss Albino mice (aged 8-10 weeks, and weight 25-30 g) were purchased from the Theodor Bilharz Research Institute, Cairo, Egypt, and maintained under standard conditions. They were housed in our animal house with 12 h /12 h of light / dark cycle maintained at a constant temperature (24 ± 2°C), relative humidity of 40–70% conditions. They were kept under specific pathogen-free conditions with free access to tap water and a standard granulated food that contained 7% simple sugars, 3% fat, 50% polysaccharide, 15% protein, and energy 3.5 kcal/g. The mice were acclimatized for 15 days prior to the experiment.

2.3. Experiment design

Fifty male Swiss albino mice were divided into three main groups: negative control mice (C, n=5), immunosuppressed uninfected mice (CS, n= 15), and immunosuppressed and infected mice (AS, n= 30). Animals of the CS and AS groups were immunosuppressed by administering 10 mg/kg of methylprednisolone sodium succinate (MPS, Solu-Medrol, Pfizer, Puurs, Belgium, Middle East) dissolved in 0.1 ml of normal saline, administered intraperitoneally for 5 days prior to *Acanthamoeba polyphaga* infection [27]. For growing *A. polyphaga* for experimental infection, 15 g of Non-nutrient agar medium (NNA) (Meron, MARINE CHEMICALS, INDIA) and Pages' amoeba saline (PAS) composed of 0.12g NaCl, 0.004g $MgSO_4.7H_2O$, 0.004g $CaCl_2.2H_2O$, 0.142g Na_2HPO_4, and 0.136g KH_2PO_4 dissolved in 1000 ml distilled water. The mixture of NNA and PAS was autoclaved and poured into Petri dishes then solidified [28]. Then, *A. polyphaga* was inoculated into a Petri dish and covered with a thin layer of heat-killed *Escherichia coli* (ATCC 25922) and then incubated at 30°C [29].Trophozoites at the exponential growth (72 to 96 hours) were collected from the petri dish, washed in phosphate-buffer saline (PBS) three times, and centrifuged at 500 ×g for 10 min/each.

The obtained pellet was suspended in PBS then a hemocytometer device was used to get the required numbers (5×10^4) equivalent to 80 µL [30]. The immunosuppressed and infected group (AS) were intravenously injected with 80 µL of *A. polyphaga* suspension via the tail vein after sterilizing it [31]. Negative control mice (C) received an equal volume of sterile saline via intravenous injection.

2.4. Re-isolation test

After scarification, fragments of kidney and lung tissues were used to enhance surface exposure and release potential microorganisms. These tissue fragments measuring approximately 5 x 5 mm were further minced into small segments and inoculated onto a Non-Nutrient Agar petri dish (NNA). Non-nutrient agar (1.5%) was prepared, with a thin overlay of *Escherichia coli* (E. coli) as a food source for the *Acanthamoeba* sp**.** Petri dishes were incubated at 28–30°C and observed daily using an inverted microscope over 14 days. This allowed for detecting the presence of trophozoites and/or cysts of amoebae [29].

To show the parasite structure, specimens from culture plates were harvested from the culture plates in a falcon tube washed twice using Phosphates buffer saline solution (CEPHAM, LIFE SCIENCE) at (500 xg) to concentrate the amoebae in the sediment. Direct unstained smear preparation as a small drop (50 µl) of the clean sediment was placed on a glass slide, covered with a coverslip to create a thin layer suitable for microscopic examination. To enhance the visualization of specific structures, 50 µl of amoeba sediment placed on a glass slide, followed by the stain such as aqueous solutions of (0.1 % methylene blue and 0.2 % Iodine), covered by a coverslip, examined under a light microscope (OPTICA, Italy) [32, 33].

2.5. Histopathology

Kidney and lung tissues were immediately excused from all groups and rinsed with NaCl 0.9 % then fixed in 10% formal alcohol for 24-48 h {30 ml of Formaldehyde of 37%, 10 ml Glacial acetic acid, and 60 ml of alcohol 95%}. The samples were processed according to the method described by Abdel-Hakeem *et al.,* 2020 [34]. Paraffin sections of 4–6 µm thickness were cut and stained with hematoxylin and eosin. The stained

sections were examined using an OPTICA microscope (Italy) equipped with a digital camera.

2.6. Renal biomarkers

About 0.1 gram of kidney tissues were homogenated in 1 ml (0.1 M) phosphate buffer (pH 7.4) using the homogenizer. The homogenates were centrifuged, and the supernatant cytosols were frozen at −20 °C for the biochemical evaluations. Tissue hemolysates were used to measure the levels of urea and creatinine. The assays were determined calorimetrically using commercial kits from Bio Diagnostic in Egypt**.**

2.7. Statistical analysis

Analyses were conducted using SPSS software (version 20). Normality of the data was evaluated using the Shapiro Wilk test, and homogeneity of variances was confirmed to ensure that the data accept the assumptions of normal distribution and equal variances. Data were tested by one-way analysis of variance (ANOVA) to compare between different groups, followed by the post- hoc test (Duncan test). Independent Samples Test (t test) used for comparing between the infected and its control group in the same period. Results are presented as mean ± standard deviation (SD)**.** A *P*-value ≤ 0.05 was considered statistically significant.

RESULTS

2.8. Re-isolation test

The re-isolation test for *A. polyphaga* from lung tissue samples showed no detectable presence of the organism in culture plates. In contrast, kidney tissue revealed a positive culture in only one mouse at 2 dpi.

The morphological structure of *A. polyphaga* trophozoites and cysts is shown in **Fig. (1)**.The trophozoites of *A. polyphaga* exhibited an irregular shape, characterized by acanthopodia, which are used for movement and feeding. The nucleus was eccentricity positioned with featured a prominent nucleolus. Additionally, the cytoplasm appeared granular due to the presence of vacuoles and other organelles. The cysts of *A. polyphaga* displayed a spherical or polygonal shape and smaller than trophozoites. They possessed a double-walled consisting of an irregular shaped outer ectocyst and a polygonal inner

endocyst. Ostioles, which serve as pores, were observed, and are thought to play a role in the excystation. The nucleus in the cysts, with a central nucleolus, resembled that of the trophozoites.

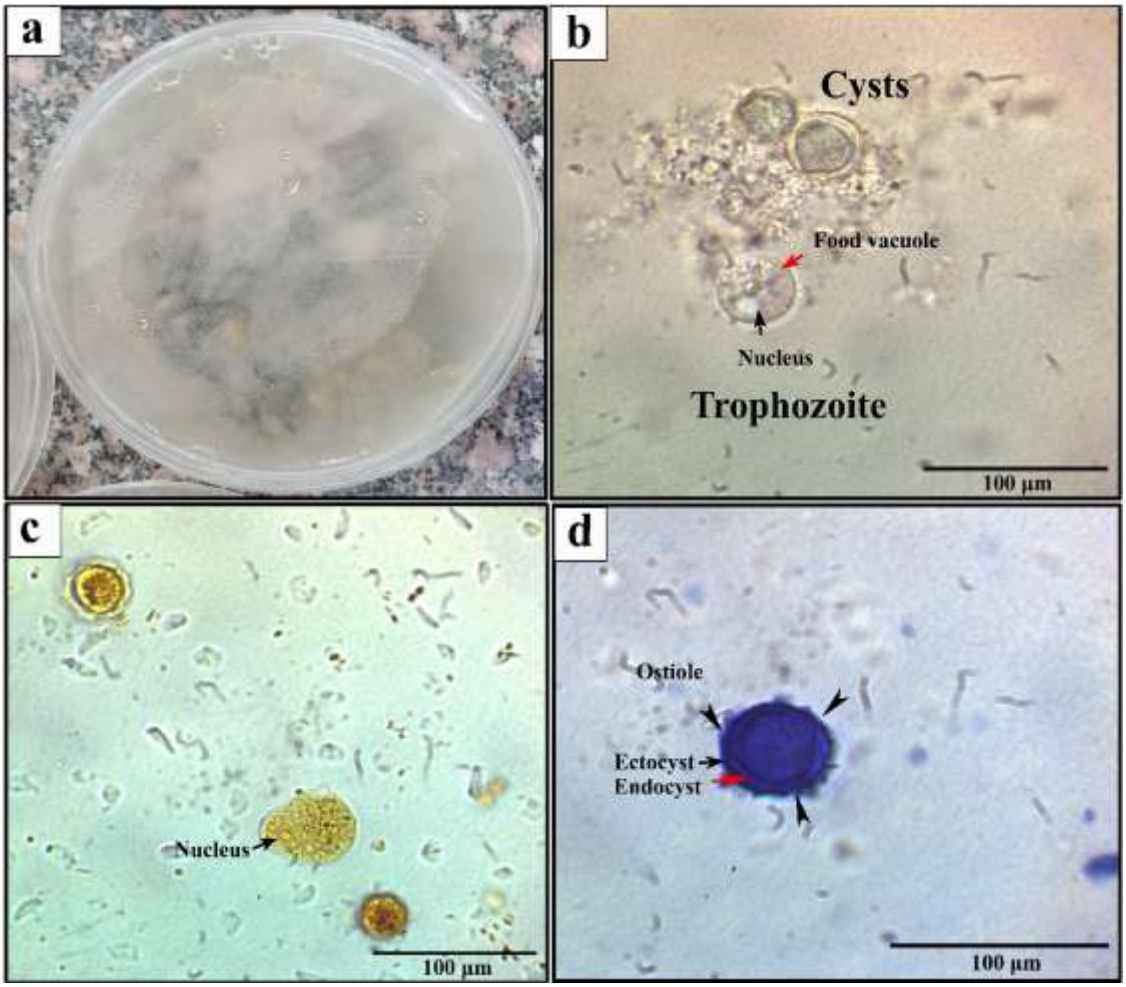

Figure (1): (a) showing culturing petri dish with fragments of kidney tissue of immunosuppressed *A. polyphaga* infected group. (b) Unstained smear showing *A. polyphaga* cysts and trophozoite. (c) Cysts and trophozoite stained with 0.2% iodine stain; (d) *A. poyphaga* cyst stained with 0.1% methylene blue. (1000 X)

2.9. Histopathology

H&E-stained kidney sections from the negative control (C) and the immunosuppressed uninfected groups (CS) at 2, 7, and 15 dpi displayed a normal renal cortex. These included glomeruli containing tufts of blood capillaries surrounded by Bowman's capsule, forming Malpighian corpuscles, as well as proximal and distal renal convoluted tubules **(Figs. 2, 3, and 4 a-b**).

In the immunosuppressed *A. polyphaga* infected group, the kidneys were mainly affected in the cortical region. At 2 dpi, inflammatory cell infiltrations consisting of macrophages, lymphocytes, and eosinophils were observed in the periglomerular and interstitial areas. Localized inflammatory cells infiltration in perivascular tissues resulted in tissue destruction, with tubules being replaced by inflammatory cells (**Fig. 2 c and d**). At 7 dpi, perivascular and interstitial inflammatory infiltration were observed, along with thrombosis in the renal vein near the corticomedullary junction (**Fig. 3 c-d**). At 15 dpi, additional changes were noted, including necrosis, pyknosis in tubular epithelial nuclei, and thrombosis in the renal vein (**Table 1, Fig. 4**). The *A. polyphaga* stages (trophozoite and cyst) were clearly observed in the periglomerular and perivascular areas at 7 and 15 dpi (**Table: 1, Fig. 4 c-d**).

Lung sections from the negative control (C) and immunosuppressed uninfected groups (CS) appeared normal bronchus, alveoli, and alveolar septa. In the infected group, numerous cysts with bilaminated walls (ecto- and endocyst) were identified in the alveolar septa **(Figs. 5, 6, 7 c-d)**. At 2 dpi, slight perivascular inflammatory cell infiltration, consisting of macrophages, lymphocytes, and eosinophils, was observed, with the alveolar septa remaining normal **(Fig. 5 c-d**). By 7 and 15 dpi, thickening of the alveolar septa, blood vessel congestion, and slight peribronchial and perivascular inflammatory infiltrations were noted **(Fig. 6 c-d)**. At 15 dpi, the thickening of the alveolar septa (interstitial pneumonia) was more pronounced compared to 7 dpi. Parasite stages were observed in the alveoli and alveolar septa, which were infiltrated by various inflammatory cells, predominantly macrophages, eosinophils, and lymphocytes (**Table 1, Fig. 7 c-d**).

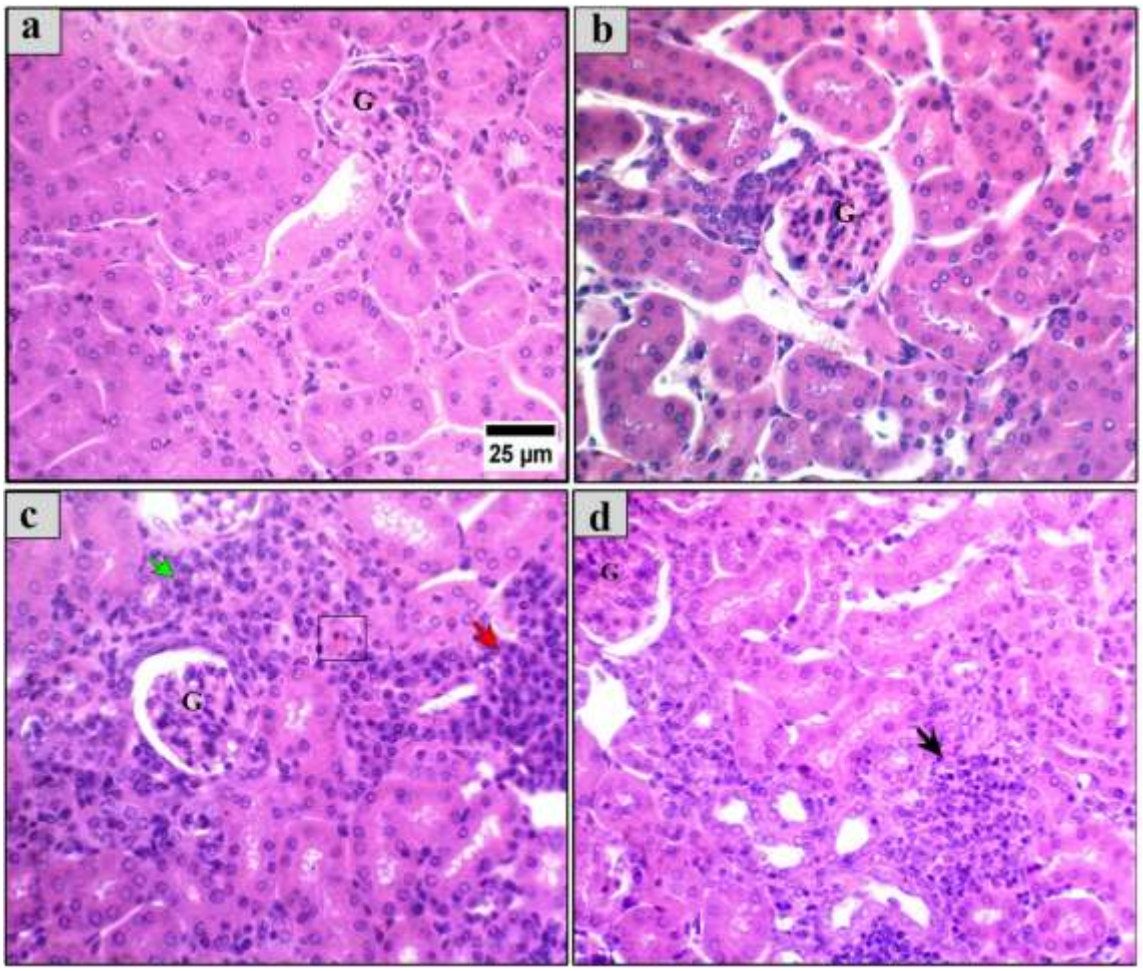

Figure (2): Histopathological section showing of mice kidney at 2 dpi, stained with H&E (400×). (a) Control negative (C). (b) Immunosuppressed uninfected (CS). (c&d) Immunosuppressed *A. polyphaga* infected (AS) showing: periglomerular (green arrow), perivascular (red arrow), and interstitial inflammatory cell infiltration (arrow); with necrotic area in the site of infiltrations. Glomeruli (G)

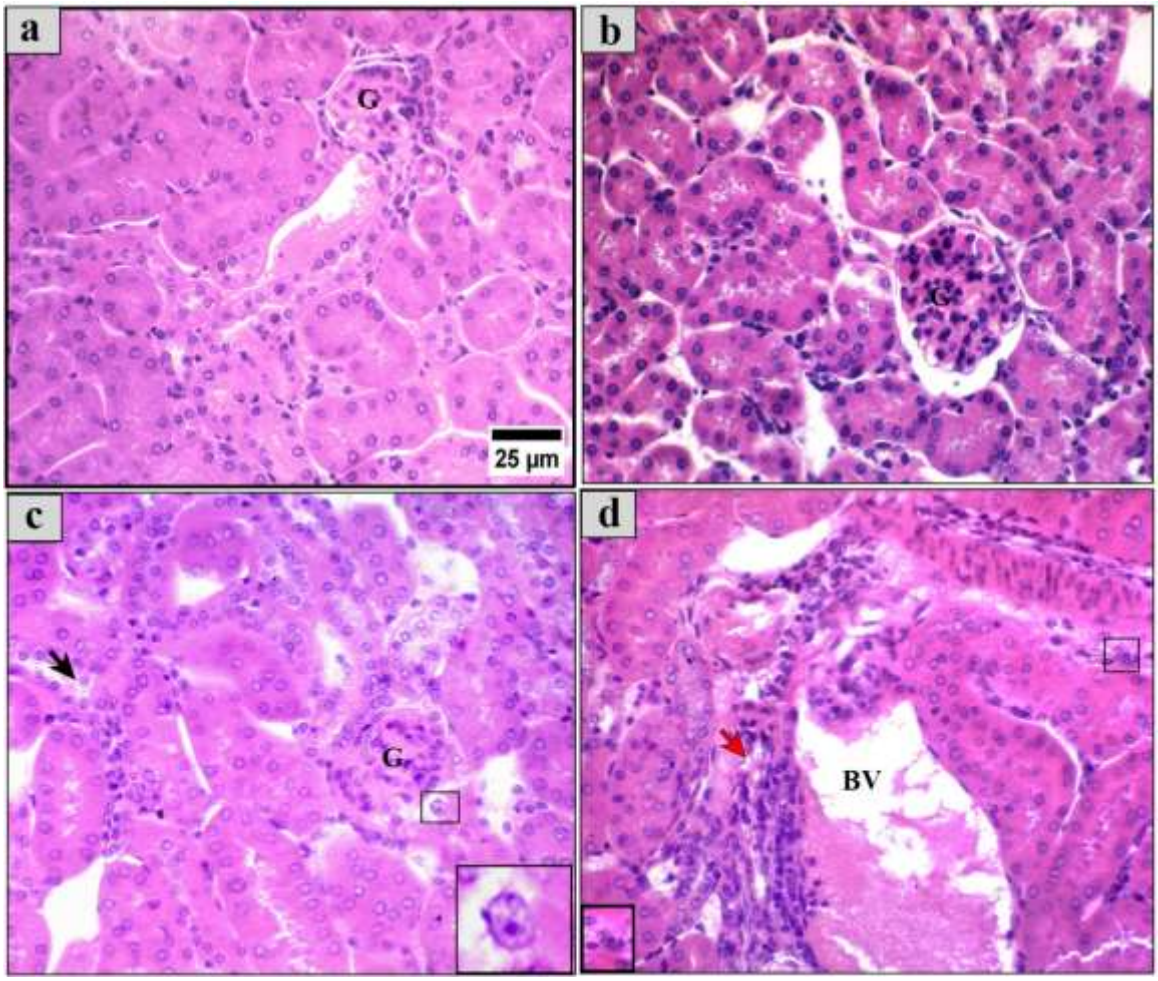

Figure (3): Histopathological section showing of mice kidney at 7 dpi, H&E (400 X). (a) Control negative (C). (b) Immunosuppressed uninfected (CS). (c&d) Immunosuppressed *A. polyphaga* infected (AS) showing: interstitial (black arrow), perivascular inflammatory cell infiltration with necrotic area in the site of infiltrations (red arrow), thrombosis in renal vein, and showing magnified trophozoites. Glomeruli (G). Blood vessel (BV).

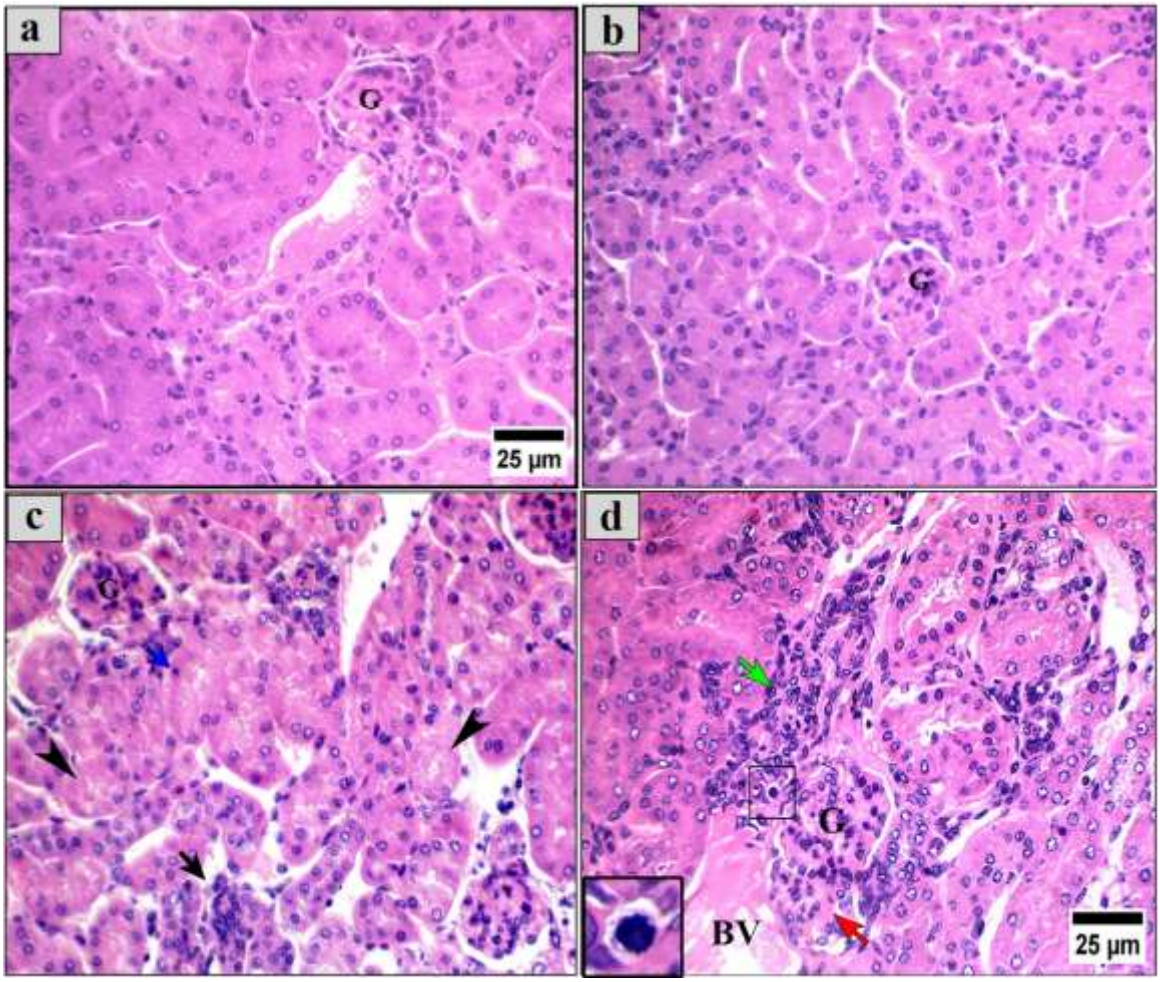

Figure (4): Histopathological section showing of mice kidney at 15 dpi, stained with H&E (400×). (a) Control negative (C). (b) Immunosuppressed uninfected (CS). (c&d) Immunosuppressed *A. polyphaga* infected (AS) showing: interstitial (black arrow), periglomerular (green arrow), perivascular inflammatory cell infiltration (red arrow), thrombosis in renal vein with magnified cyst, necrosis (head arrow), and pyknosis (blue arrow). Glomeruli (G). Blood vessel (BV).

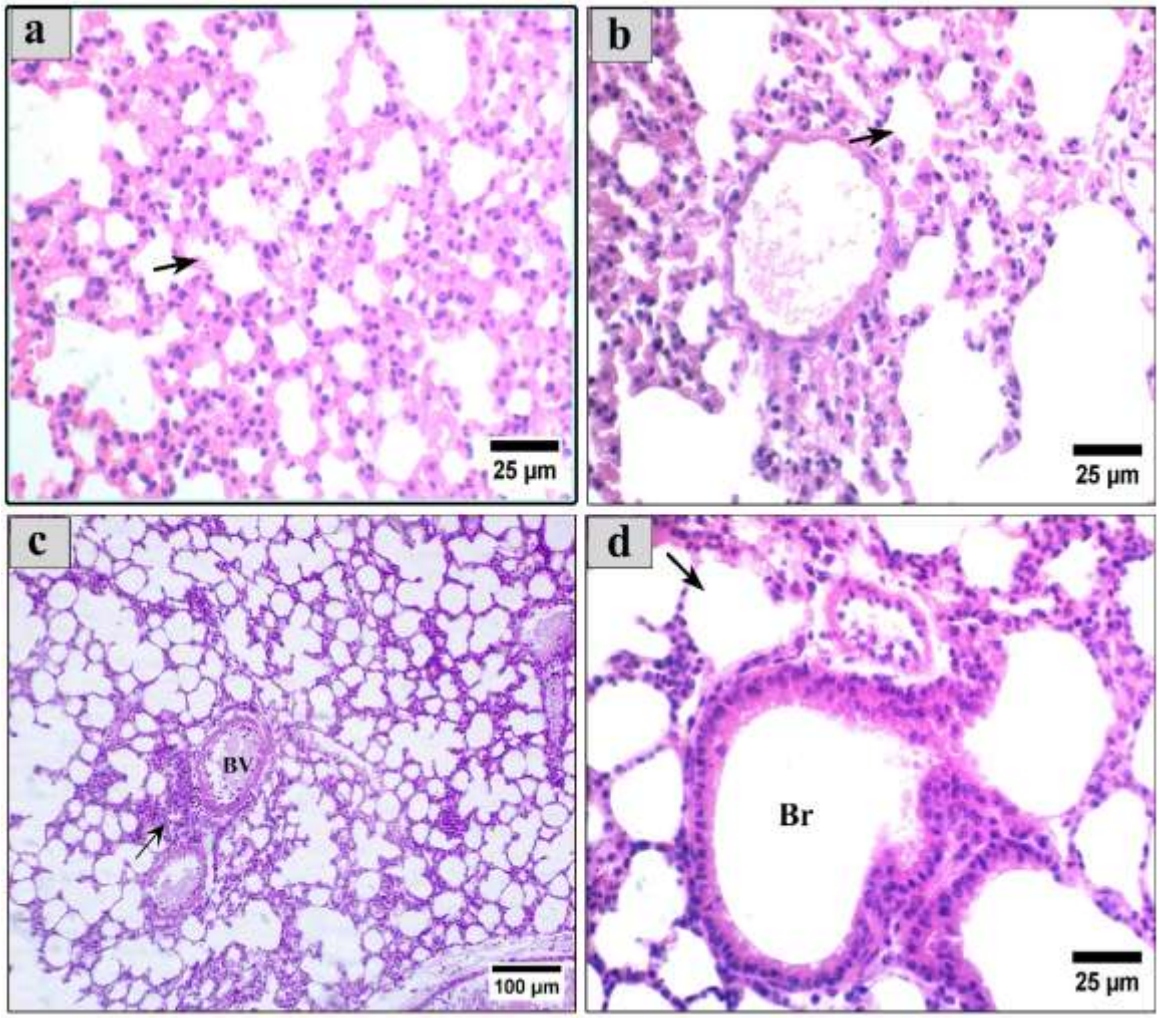

Figure (5): Histopathological section showing of mice lung at 2 dpi, stained with H&E (400×). (a) Control negative (C). (b) Immunosuppressed uninfected (CS). (c&d) Immunosuppressed & *A. polyphaga* infected (AS) showing: Perivascular inflammatory infiltration (arrow) and normal alveolar wall (arrow). BV: blood vessel. Br: bronchus.

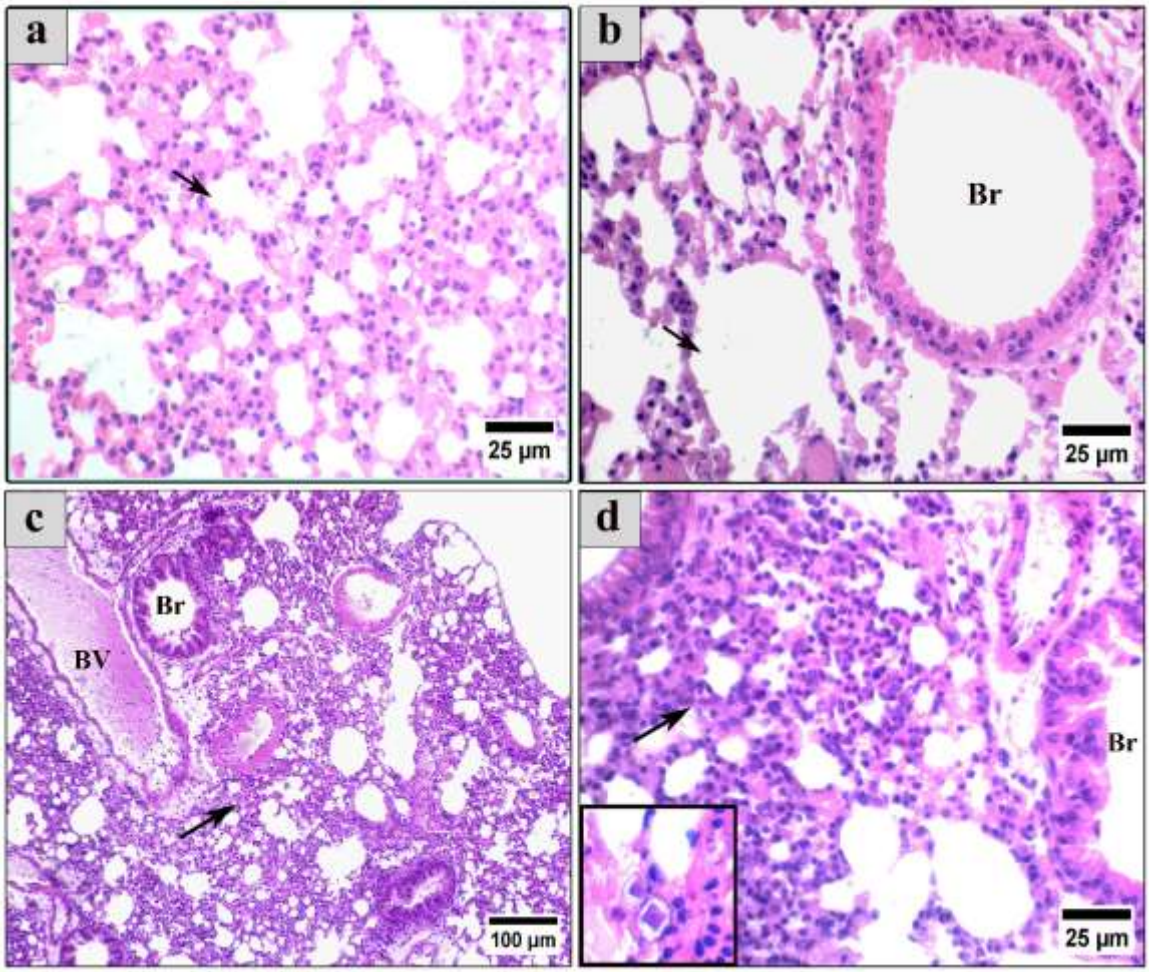

Figure (6): Histopathological section showing of mice lung at 7 dpi, stained with H&E (400×). (a) Control negative (C). (b) Immunosuppressed uninfected (CS). (c & d) Immunosuppressed *A. polyphaga* infected (AS) *showing*: slight thickening in the alveolar wall (arrow) and congestion in the blood vessel (BV) with parasite cyst in alveolar septae (box). BV: blood vessel. Br: bronchus.

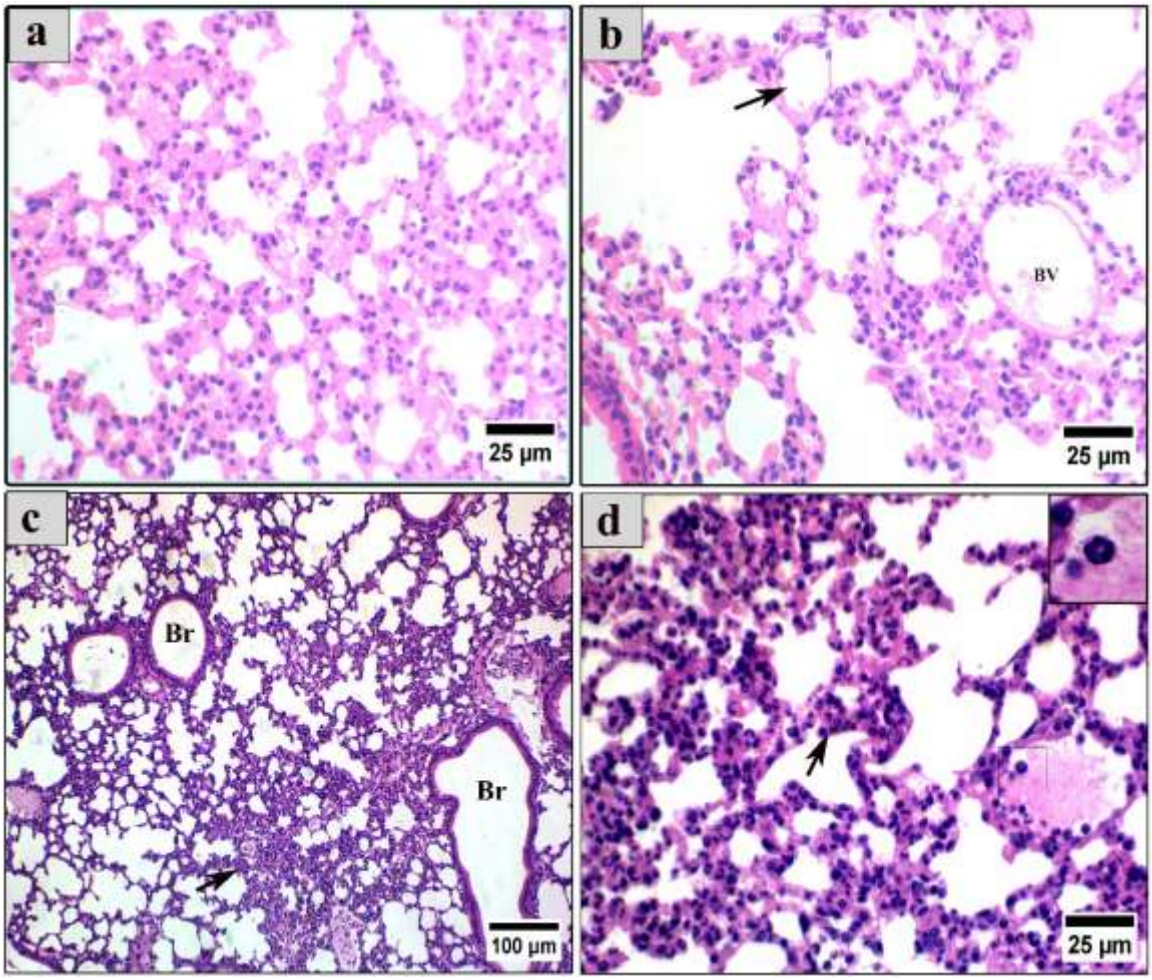

Figure (7): Histopathological section showing of mice lung at 15 dpi, stained with H&E (400×). (a) Control negative (C). (b) Immunosuppressed uninfected (CS). (c & d) Immunosuppressed *A. polyphaga* infected (AS) showing thickening in the alveolar wall (arrow) with the presence of parasite cyst (magnified). Br: bronchus.

Table 1: Showed scores of the histopathological changes in the kidney and lung tissues in all experimental groups.

Group / Parameters	C	CS (2,7, and 15 days)	AS 2 dpi	AS 2 dpi	AS 15 pi
a. Kidney					
Perivascular inflammatory infiltration	-	-	++	++	++
Perigromerular inflammatory infiltration	-	-	+	+	++
Interstitial inflammatory infiltration	-	-	++	++	++
Thrombosis in the renal vein.	-	-	+	+	+
Necrosis in tubular epithelium	-	-	+	+	++
Necrosis in glomerular tuft	-	-	+	+	+
a. Lung					
Perivascular inflammatory infiltration	-	-	+	+	++
Peribronchial inflammatory infiltration	-	-	+	++	++
Thickening in alveolar septae	-	-	-	++	+++
Congestion in blood vessels	-	-	-	+	+

Score: (-) absent; (+) mild; (++) moderate; and (+++) severe.

C: control negative. CS: immunosuppressed uninfected animals. AS: immunosuppressed &*A. polyphaga* animals.

2.10. Renal function biomarkers

For urea and creatinine, a statistically significant difference was observed between the different groups (P= 0.009 and P= 0.000, respectively). In the AS group, there was a highly significant increase in both urea and creatinine levels at 7 dpi compared to the CS group (t= 5.16, P=0.02 for urea; t= 35.63, P=0.000 for creatinine). Similarly, at 15 dpi, urea and creatinine levels in the AS group were significantly higher compared to the CS group (t= 6.932, P=0.002 for urea; t= 7.16, P=0.002 for creatinine) (**Fig. 8 a-b**).

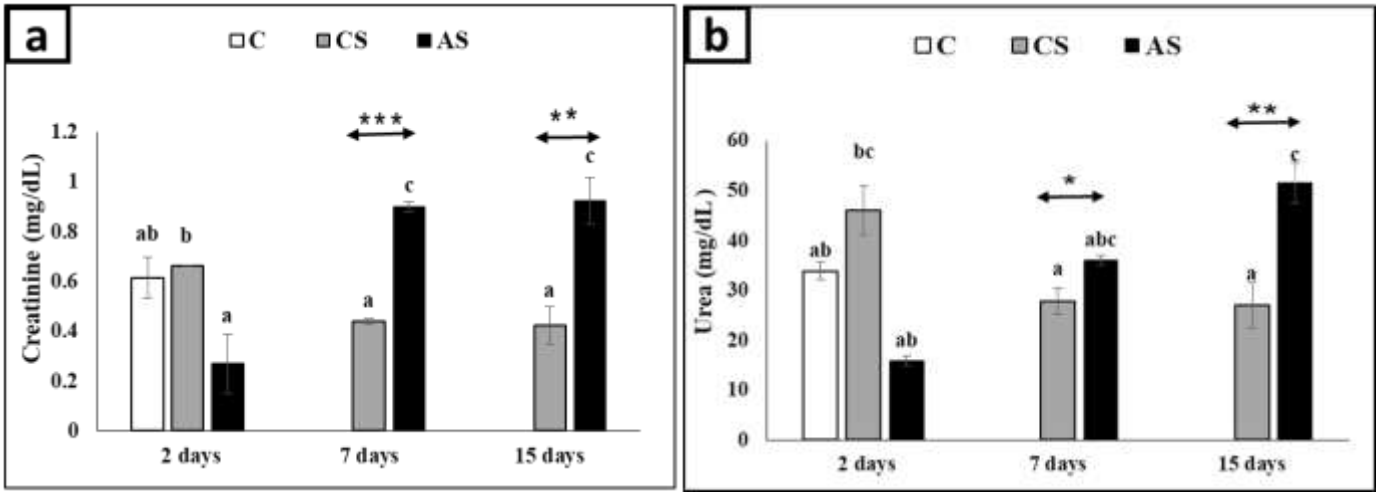

Figure (8): Histogram illustrating both (a) Creatinine and (b) Urea level in all experimental groups at 2, 7, and 15 dpi. (*) indicate a significant difference at $P \leq 0.05$, (**) at $P \leq 0.001$, and (***) a highly significance at $P \leq 0.0001$. C: control negative. CS: immunosuppressed uninfected animals. AS: immunosuppressed &*A. polyphaga* animals.

DISCUSSION

This study investigated the pathogenicity of systemic infection induced by *Acanthamoeba polyphaga* isolated from contaminated contact lenses and its impact on the kidneys and lungs of immunosuppressed mice. The methods employed included histopathological analysis, re-isolation techniques, and biochemical parameter assessments. The pathogenicity of *Acanthamoeba* species varies among strains and has been classified by Ramirez *et al.,* 2006 [35] into pathogenic, invasive, and non-pathogenic. *Acanthamoeba polyphaga* demonstrated its pathogenicity in disseminated Acanthamoebisais through histopathological changes and positive re-isolation from the kidneys of infected mice. Similarly, Alves *et al.* 2016 [15] illustrated the pathogenicity of *A. polyphaga* (ATCC 30461) following intraperitoneal inoculation in experimental immunocompetent animals, with positive re-isolation from brain and kidney tissues. In addition, Omaña-Molina *et al.,* 2017 [36] reported re-isolation of *A. castellanii* from various organ samples such as brain, lung, liver, and kidney without causing mortality in the inoculated mice and *A. culbertsoni* showed positive re-isolated from brain and lung only with caused 50% mortality.

Acanthamoebiasis is predominantly observed in immunocompromised individuals, with immunosuppressive drugs facilitating the spread of the infection [9]. Due to the challenges in biochemical analysis in disseminated acanthamoebiasis, post-mortem histopathological examination and amoebae re-isolation from infected hosts are the primary methods employed to confirm the infection [37]. Since the kidneys are vital detoxification organs, the inflammation process can alter blood biochemical indicators, notably affecting critical renal function markers like urea and creatinine [38]. This study revealed significant alterations in renal biochemical markers. Specifically, urea and creatinine levels decreased compared to controls on day 2 post-infection but increased significantly by days 7 and 15 post-infection. Despite these changes, *A. polyphaga* was re-isolated from the kidneys of mice with normal renal function [27, 37]. Notably, patients with disseminated *Acanthamoeba* infections often exhibit normal levels of urea, creatinine, and liver function enzyme activities [39, 40]. Discrepancies in results could be attributed to differences in incubation periods, infection routes, *Acanthamoeba* sp. strain, and host immunity [1].

Acanthamoeba polyphaga disseminated haematogenously to several organs, including the kidneys and lungs, triggering an inflammatory cell infiltration during the early stages of infection (within the first 15 days), this contrasts with findings reported by Omaña-Molina *et al.,* 2017 [36]. This study suggests that *A. polyphaga* not only reaches the kidney via hematogenous routes but also establishes its presence in renal tissues, inducing progressive pathological changes, particularly in the cortical region. At 2 and 7 dpi, inflammatory cell infiltration was observed in periglomerular, perivascular, and interstitial areas, and congestion in the renal vein. By 15 dpi, necrosis became more evident, with a distinct distribution of *A. polyphaga* stages identified in the periglomerular and perivascular tissues. The environmental strains of *Acanthamoeba* spp. have shown similar effects on kidney tissue during early infection in experimental animals [41, 42]. Additionally, Alves *et al.,* 2016 [15] reported significant histopathological changes in the livers, kidneys, and lungs of rats infected intracranially and/or intraperitoneally with the *Acanthamoeba* T4 genotype. Differences in the impact on host kidneys might be attributed to the specific *Acanthamoeba* strain involved [41]. Interestingly, Omaña-Molina *et al.,* 2017 [36], proposed that *A. castellanii* trophozoites

invaded renal tissue through renal tubules, residing between the cell junctions, while *A. culbertsoni* was not detected in the kidneys of infected mice.

Acanthamoeba spp. induce allergic airway symptoms in mice, potentially reflecting similar occurrences in humans [24]. In this study, normal lung sections was observed at 2 dpi, with slight perivascular inflammatory infiltration. By 7 and 15 dpi, interstitial pneumonia, mild peribronchial and perivascular inflammatory infiltrations, congestion in blood vessels, and parasite distribution in the alveolar septa and alveoli were evident. These findings align with Lanocha *et al.*, 2009 [43], who isolated *Acanthamoeba* spp. from bronchoaspirate samples of immunosuppressed patients exhibiting typical pneumonia symptoms. Furthermore, *Acanthamoeba castellanii* trophozoites were detected in alveolar spaces 24 h post-inoculation, surrounded by macrophages [36]. Other studies have reported pulmonary parenchymal damage, bronchial epithelium hyperplasia, blood vessel destruction, and inflammatory cell infiltration in experimental *Acanthamoeba* spp. infections [42, 44, 45]. The degree of inflammation may depend on the infection dosage and host immune status [24, 44].

This study demonstrated the pathogenic potential of *Acanthamoeba polyphaga* isolated from contact lenses, highlighting its severe effects on immunosuppressed animals as evidenced by histopathological changes and re-isolation test. The progression of the infection may be influenced by factors such as the host's immune condition, the inoculation route, infection dose, and the genetic variability of the strain [13].

CONCLUSION

A. polyphaga poses a significant risk to immunocompromised individuals, with its ability to cause disseminated infection and severe organ-specific histopathology. These findings underscore the importance of further research into the mechanisms of *Acanthamoeba* dissemination, host-pathogen interactions, and potential therapeutic interventions.

REFERENCES

[1] K. Kot, D. Kosik-Bogacka, M. Ptak, P. Roszkowska, A. Kram, Histological changes in the kidneys and heart in experimental Acanthamoebiasis in immunocompetent and immunosuppressed hosts, Folia Biologica (Kraków), 69 (2021) 167.

[2] A.-H. Ahmad, M. Bahgat, A.-E. Mohammed, A. Ashour, W. Hikal, *Acanthamoeba* species in swimming pools of Cairo, Egypt, Iran J Parasitol, 9 (2014) 194.

[3] A.Z. Al-Herrawy, M.A. Marouf, M.A. Gad, *Acanthamoeba* species in tap water, Egypt, Int J Clin Pharma Res, 9 (2017) 1.

[4] R. Elseadawy, I. Abbas, M. Al-Araby, S. Abu-Elwafa, Occurrence and molecular characterization of *Acanthamoeba*, *Naegleria fowleri* and *Blastocystis* in water samples from various sources in Egypt, Acta Trop, 237 (2023) 106733.

[5] A. Hassan, H. Farouk, F. Hassanein, R. Abdul-Ghani, A.H. Abdelhady, *Acanthamoeba* contamination of hemodialysis and dental units in Alexandria, Egypt: A neglected potential source of infection,J Infect Public Health, 5 (2012) 304.

[6] F.A. Hassan, M. Tolba, G.H. Abed, H. Omar, S.S. Abdel-Hakeem, Contact lenses contamination by *Acanthamoeba* spp. In upper Egypt, PLoS. ONE 16 (2021) e0259847.

[7] E.E. Taher, E.M. Méabed, I. Abdallah, W.Y.A. Wahed, Acanthamoeba keratitis in noncompliant soft contact lenses users: Genotyping and risk factors, a study from Cairo, Egypt, J Infect Public Health, 11 (2018) 377.

[8] B. Clarke, A. Sinha, D.N. Parmar, E. Sykakis, Advances in the diagnosis and treatment of Acanthamoeba Keratitis, J Ophthalmol, 2012 (2012).

[9] M.N. Brondfield, M.J. Reid, R.L. Rutishauser, J.R. Cope, J. Tang, J.M. Ritter, A. Matanock, I. Ali, S.B. Doernberg, A. Hilts- Horeczko, Disseminated *Acanthamoeba* infection in a heart transplant recipient treated successfully with a miltefosine- containing regimen: Case report and review of the literature, Transpl Infect Dis, 19 (2017) e12661.

[10] K. Kot, N. Lanocha-Arendarczyk, D.I. Kosik-Bogacka, Amoebas from the genus *Acanthamoeba* and their pathogenic properties, Ann Parasitol, 64 (2018) 299.

[11] N. Łanocha-Arendarczyk, D. Kosik-Bogacka, K. Galant, W. Zaorski, K. Kot, A. Łanocha, Pathogenic free-living amoeba, POST. MIKROBIOL, 56 (2017) 106.

[12] A. Kutner, M. Aldrich, S. Patel, J.J. Kang, B. Amin, R. Mann, I.K.M. Ali, R.B. Martines, J.R. Cope, G.O. De Boccardo, *Acanthamoeba* endophthalmitis during treatment for cutaneous disease in a renal transplant patient,Transpl Infect Dis, 20 (2018) e12843.

[13] F. Marciano-Cabral, G. Cabral, *Acanthamoeba* spp. as agents of disease in humans, Clin Microbiol Rev,16 (2003) 273.

[14] A.J. Martinez, G.S. Visvesvara, Free- living, amphizoic and opportunistic amebas, Brain Pathol, 7 (1997) 583.

[15] D.d.S.M.M. Alves, A.S. Moraes, L.M. Alves, R. Gurgel-Gonçalves, R.d.S. Lino Junior, C.A. Cuba-Cuba, M.C. Vinaud, Experimental infection of T4 *Acanthamoeba* genotype determines the pathogenic potential, Parasitol Res, 115 (2016) 3435.

[16] A. Salahuldeen, A. El-Aziz, M. A Gad, M. F Abou-El Nour, A. Z Al-Herrawy, Potentially pathogenic free-living amoebae in fresh and sea waters from Alexandria, Egypt, EJABF, 24 (2020) 307.

[17] B. Schwartz, S. Mawhorter, Parasitic infections in solid organ transplantation, Am J Transplant, 13 (2013) 280.

[18] A. Young, N. Leboeuf, S. Tsiouris, S. Husain, M. Grossman, Fatal disseminated *Acanthamoeba* infection in a liver transplant recipient immunocompromised by combination therapies for graft- versus- host disease, Transpl Infect Dis, 12 (2010) 529.

[19] G.E. Khalife, S.E. Pambuccian, G.S. Visvesvara, B. Horten, Disseminated *Acanthamoeba* infection masquerading as bacillary angiomatosis in a patient with aids: Case report and literature review, Int. J. Surg. Pathol, 2 (1994) 11.

[20] K.I. Im, D.S. Kim, Acanthamoebiasis in Korea: Two new cases with clinical cases review, Yonsei Med J, 39 (1998) 478.

[21] S. Vernon, B. Acar, S. Pham, D. Fertel, *Acanthamoeba* infection in lung transplantation: Report of a case and review of the literature, Transpl Infect Dis, 7 (2005) 154.

[22] O. Ringsted, B.V. Jager, D. Suk, G.S. Vlsvesvara, Probable *Acanthamoeba* meningoencephalitis in a Korean child, Am J Clin Pathol, 66 (1976) 723.

[23] B. Rodríguez-Iturbe, E.A. Burdmann, R.S. Barsoum, Glomerular diseases associated with infection, Comprehensive clinical nephrology (2010) 662.

[24] M.K. Park, M.K. Cho, S.A. Kang, H.-K. Park, D.-H. Kim, H.S. Yu, *Acanthamoeba* protease activity promotes allergic airway inflammation via protease-activated receptor 2, PLoS. ONE 9 (2014) e92726.

[25] R. Siddiqui, N.A. Khan, Biology and pathogenesis of *Acanthamoeba*, Parasites & vectors 5 (2012) 1.

[26] N.P. Du Sert, A. Ahluwalia, S. Alam, M.T. Avey, M. Baker, W.J. Browne, A. Clark, I.C. Cuthill, U. Dirnagl, M. Emerson, Reporting animal research: Explanation and elaboration for the arrive guidelines 2.0, PLoS biol, 18 (2020) e3000411.

[27] N. Łanocha-Arendarczyk, I. Baranowska-Bosiacka, K. Kot, B. Pilarczyk, A. Tomza-Marciniak, J. Kabat-Koperska, D. Kosik-Bogacka, Biochemical profile, liver and kidney selenium (se) status during Acanthamoebiasis in a mouse model, Folia Biologica (Kraków) 66 (2018) 33.

[28] Z.A. Polat, S. Ozcelik, A. Vural, E. Yıldız, A. Cetin, Clinical and histologic evaluations of experimental Acanthamoeba keratitis, Parasitol Res, 101 (2007) 1621.

[29] S.S. Abdel-Hakeem, H.E.-d.M. Omar, G.H. Abed, F.A.M. Hassan, O. Al-Bedak, M.E.M. Tolba, Bioactive compounds of *ziziphus spina-christi* seeds extract and cellulase enzyme attenuates the growth of *Acanthamoeba polyphaga* isolated from contact lenses, EAJBSZ, 13 (2021) 307.

[30] D.d.S.M.M. Alves, R. Gurgel-Gonçalves, P. Albuquerque, C.A. Cuba-Cuba, M.I. Muniz-Junqueira, S.A.S. Kückelhaus, A method for microbial decontamination of *Acanthamoeba* cultures using the peritoneal cavity of mice, Asian Pac J Trop Biomed, 5 (2015) 796.

[31] C. Culbertson, J. Smith, H. Cohen, J. Minner, Experimental infection of mice and monkeys by *Acanthamoeba*, Am J Pathol, 35 (1959) 185.

[32] N.M. El-Sayed, W.M. Hikal, Several staining techniques to enhance the visibility of *Acanthamoeba* cysts, Parasitol Res, 114 (2015) 823.

[33] J. Lorenzo-Morales, N.A. Khan, J. Walochnik, An update on Acanthamoeba keratitis: Diagnosis, pathogenesis and treatment, Parasite 22 (2015).

[34] S.S. Abdel-Hakeem, M.A. Abdel-Samiee, G.H. Abed, An insight into the potential parasitological effect of *Schistosoma mansoni* antigens in infected mice: Prophylactic role of cercarial antigen, Microsc Microanal, 26 (2020) 708.

[35] E. Ramirez, E. Campoy, D. Matuz, E. Robles, *Acanthamoeba* isolated from contaminated groundwater, J Eukaryot Microbiol, 53 (2006) S10.

[36] M. Omaña-Molina, D. Hernandez-Martinez, R. Sanchez-Rocha, U. Cardenas-Lemus, C. Salinas-Lara, A.R. Mendez-Cruz, L. Colin-Barenque, P. Aley-Medina, J. Espinosa-Villanueva, L. Moreno-Fierros, In vivo CNS infection model of *Acanthamoeba* genotype T4: The early stages of infection lack presence of host inflammatory response and are a slow and contact-dependent process, Parasitol Res, 116 (2017) 725.

[37] K. Kot, D. Kosik-Bogacka, A. Wojtkowiak-Giera, A. Kolasa-Wołosiuk, N. Łanocha-Arendarczyk, The expression of TLR 2 and TLR 4 in the kidneys and heart of mice infected with *Acanthamoeba* spp, Parasites & Vectors 13 (2020) 1.

[38] D.S. Gardner, J.C. Allen, D. Goodson, D. Harvey, A. Sharman, H. Skinner, A. Szafranek, J.S. Young, E.H. Bailey, M.A. Devonald, Urinary trace elements are biomarkers for early detection of acute kidney injury, Kidney Int Rep, 7 (2022) 1524.

[39] R. Tilak, R. Singh, I. Wani, A. Parekh, J. Prakash, U. Usha, An unusual case of *Acanthamoeba peritonitis* in a malnourished patient on continuous ambulatory peritoneal dialysis (capd), J Infect Dev Ctries, 2 (2008) 146.

[40] D. Webster, I. Umar, G. Kolyvas, J. Bilbao, M.-C. Guiot, K. Duplisea, Y. Qvarnstrom, G.S. Visvesvara, Case report: Treatment of granulomatous amoebic encephalitis with voriconazole and miltefosine in an immunocompetent soldier, Am J Trop Med Hyg, 87 (2012) 715.

[41] M.T. Frade, L.F.d. Melo, C.R. Pessoa, J.L.d. Araújo, R.A. Fighera, A.P. Souza, F. Uzal, A.F. Dantas, Systemic Acanthamoebiasis associated with canine distemper in dogs in the semiarid region of paraíba, brazil, Pesq. Vet. Bras, 35 (2015) 160.

[42] K. Górnik, W. Kuźna-Grygiel, Histological studies of selected organs of mice experimentally infected with *Acanthamoeba* spp, Folia Morphol (Warsz), 64 (2005) 161.

[43] N. Lanocha, D. Kosik-Bogacka, A. Maciejewska, M. Sawczuk, A. Wilk, W. Kuzna-Grygiel, The occurrence *Acanthamoeba* (free-living amoeba) in environmental and respiratory samples in Poland, Acta Protozool, 48 (2009) 271.

[44] I.-T. Lee, C.-M. Yang, Inflammatory signalings involved in airway and pulmonary diseases, Mediators Inflamm, 2013 (2013).

[45] R. Martínez-Girón, J. Esteban, A. Ribas, L. Doganci, Protozoa in respiratory pathology: A review, Eur Respir J, 32 (2008) 1354.